COMPUTATIONAL SCIENCE&DISCOVERY

The nuclear force from Monte Carlo simulations of lattice quantum chromodynamics

S Aoki[1,2], **T Hatsuda**[3] **and N Ishii**[4]

[1] Graduate School of Pure and Applied Sciences, University of Tsukuba, 1-1-1 Tennodai, Tsukuba 305-8571, Japan
[2] RIKEN BNL Research Center, Brookhaven National Laboratory, Upton, NY 11973, USA
[3] Department of Physics, The University of Tokyo, 7-3-1 Hongo, Bunkyo-ku, Tokyo 113-0033, Japan
[4] Center for Computational Sciences, University of Tsukuba, 1-1-1 Tennodai, Tsukuba 305-8571, Japan
E-mail: saoki@het.ph.tsukuba.ac.jp, hatsuda@phys.s.u-tokyo.ac.jp and ishii@rarfaxp.riken.jp

Received 16 May 2008, in final form 26 September 2008
Published 20 November 2008
Computational Science & Discovery **1** (2008) 015009 (11pp)
doi:10.1088/1749-4699/1/1/015009

Abstract. The nuclear force acting between protons and neutrons is studied in the Monte Carlo simulations of the fundamental theory of strong interaction, the quantum chromodynamics defined on the hypercubic space–time lattice. After a brief summary of the empirical nucleon–nucleon (NN) potentials that can fit the NN scattering experiments in high precision, we outline the basic formulation for deriving the potential between the extended objects such as the nucleons composed of quarks. The equal-time Bethe–Salpeter (BS) amplitude is a key ingredient for defining the NN potential on the lattice. We show the results of the numerical simulations on a 32^4 lattice with lattice spacing $a \simeq 0.137$ fm (lattice volume $(4.4\,\text{fm})^4$) in the quenched approximation. The calculation was carried out using the massively parallel computer Blue Gene/L at the High Energy Accelerator Research Organization (KEK). We found that the calculated NN potential at low energy has the basic features expected from the empirical NN potentials: attraction at long and medium distances, and the repulsive core at short distances. Various future directions along this line of research are also summarized.

Contents

1. Introduction

One of the long standing problems in particle and nuclear physics is the origin of the strong nuclear force that holds the nucleons (protons and neutrons) inside atomic nuclei. For the past half century, phenomenological fits of the proton–proton (pp) and neutron–proton (np) scattering data assuming empirical nucleon–nucleon (NN) potentials have been attempted [1][5]: the potentials, which can fit more than 2000 data points of the NN phase shift with $\chi^2/\mathrm{dof} \simeq 1$ for $T_{\mathrm{lab}} < 300\,\mathrm{MeV}$, include the CD-Bonn potential [3], Argonne v_{18} potential [4] and Nijmegen potentials [5]. An alternative approach based on the chiral perturbation theory has been also developed [6].

In figure 1, three examples of the empirical NN potentials in the ${}^1S_0$ channel are shown[6]. From this figure, some characteristic features of the nuclear force can be identified.

I. The long range part of the nuclear force ($r > 2$ fm) is dominated by the one-pion exchange originally introduced by Yukawa [8].

II. The medium range part (1 fm $< r <$ 2 fm) receives significant contributions from the exchange of multi-pions and heavy mesons (ρ, ω and σ). In particular, the spin–isospin-independent attraction of about -50 to -100 MeV in this region plays an essential role in binding the atomic nuclei.

III. The short range part ($r < 1$ fm) behaves as a repulsive core originally introduced by Jastrow [9] to explain the pp and np scattering phase shifts simultaneously. Such a short range repulsion is relevant to the stability of atomic nuclei, to the maximum mass of neutron stars and to the ignition of the Type II supernova explosions [10].

It is now well established that the nucleons are made of quarks and gluons, which obey the law of quantum chromodynamics (QCD) [11]. Therefore, it is tempting to derive the strong nuclear force from the quark–gluon degrees of freedom. Two nucleons have a sizable overlap at distance $r < 1$ fm since the proton's charge radius is about 0.86 fm. Therefore, the nuclear force at short distances must be described by taking into account the direct exchange of the quarks and gluons between the nucleons. So far, there have been numerous theoretical attempts to understand the nuclear force from the quark structure of the nucleon[7]. However, conclusive results have not been obtained because of the highly non-perturbative nature of QCD.

Recently, we developed a new approach to this long-standing problem of nuclear force on the basis of QCD defined on a space–time lattice, the lattice QCD (LQCD) [13, 14]. In LQCD, physical quantities are expressed by highly multi-dimensional integrals, which can be carried out by the importance sampling method. Our aim was to define the NN potential in the coordinate space from the equal-time Bethe–Salpeter (BS) amplitude calculated on the lattice: the first results on the central NN potential in the ${}^1S_0$ and ${}^3S_1$

[5] The NN and hyperon–nucleon (YN) scattering data are compiled in [2].

[6] A system of two nucleons with total spin $s = (0, 1)$, orbital angular momentum $L = (S, P, D, \ldots)$ and total angular momentum $J = (0, 1, 2, \ldots)$ is denoted by ${}^{2s+1}L_J$.

[7] Reviewed in [12].

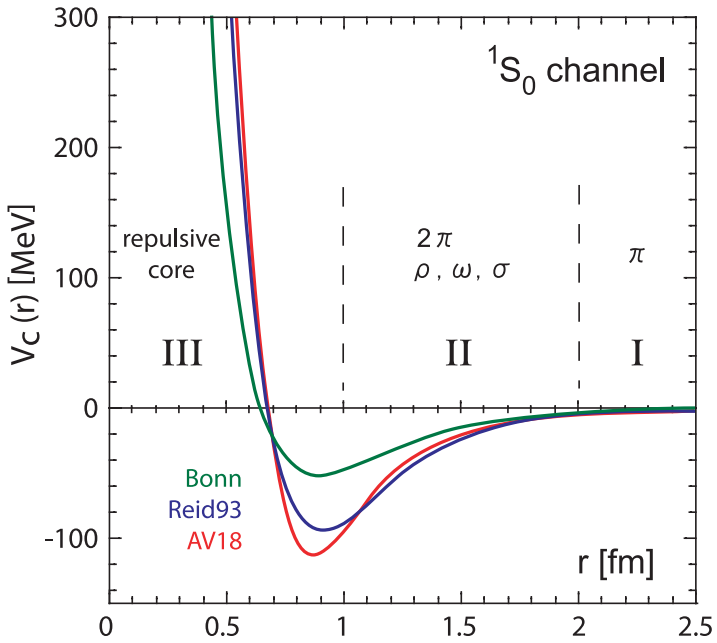

Figure 1. Three examples of the high-precision NN potentials in the ${}^1S_0$ channel. AV18 stands for the Argonne v_{18} potential [4], Reid93 stands for one of the Nijmegen potentials [5] and Bonn stands for the Bonn potential [7]. I, II and III correspond to the long range part, the medium range part and the short range part, respectively, as discussed in the text.

channels have been reported with the quenched lattice QCD simulations in [15–17]. Also, the first results on the hyperon–nucleon (YN) potential have been reported in [18, 19].

In the following, we will outline the field theoretical derivation of the NN potential from QCD [20] in sections 2 and 3. Then, we show how to define the potential in LQCD formalism in section 4. The basic setup and the method of our numerical simulations are described in section 5. Some numerical results on the low-energy NN potential taken from [15, 16] are presented in section 6. The last section is devoted to the summary and concluding remarks with a discussion on future directions.

2. The Bethe–Salpeter wavefunction

Let us start with the definition of the BS amplitude for the proton–neutron system,

$$\Psi_{\alpha\beta}(x, y) = \langle 0|\mathrm{T}[\hat{n}_\beta(y)\hat{p}_\alpha(x)]|\mathrm{p}(\vec{q}, s)\mathrm{n}(\vec{q}', s'); \mathrm{in}\rangle, \tag{1}$$

$$\hat{n}_\beta(y) = \varepsilon_{abc}\left(\hat{u}_a(y)C\gamma_5\hat{d}_b(y)\right)\hat{d}_{c\beta}(y), \tag{2}$$

$$\hat{p}_\alpha(x) = \varepsilon_{abc}\left(\hat{u}_a(x)C\gamma_5\hat{d}_b(x)\right)\hat{u}_{c\alpha}(x), \tag{3}$$

where $(\vec{q}, s)$ and $(\vec{q}', s')$ denote the spatial momentum and the spin state of the incoming proton and those of the neutron, respectively. The local composite operator for the neutron (proton) is denoted by $\hat{n}_\beta(y)$ $(\hat{p}_\alpha(x))$ with the operators for the up-quark $\hat{u}(x)$ and the down-quark $\hat{d}(x)$. Also, α and β denote the Dirac indices, a, b and c the color indices, and C the charge conjugation matrix in the spinor space.

One of the advantages of using the local operator for the nucleon is that the Nishijima and Zimmermann (NZ) reduction formula [21] for local composite fields can be utilized. In particular, in and out nucleon fields are defined through the Yang–Feldman equation,

$$\sqrt{Z}\hat{N}_{\mathrm{in/out}}(x) = \hat{N}(x) - \int S_{\mathrm{adv/ret}}(x - x'; m_{\mathrm{N}})\hat{J}(x')\mathrm{d}^4x', \tag{4}$$

where $\hat{N}(x)$ is the nucleon composite operator ($\hat{n}(x)$ or $\hat{p}(x)$ in equations (2) and (3)), $\hat{N}_{\rm in/out}(x)$ is the associated in/out field, $m_{\rm N}$ is the physical nucleon mass, and $\hat{J}(x) \equiv (\mathrm{i}\partial\!\!\!/_x - m_{\rm N})\hat{N}(x)$. The advanced/retarded propagator for the free nucleon field with the mass $m_{\rm N}$ is denoted by $S_{\rm adv/ret}(x - x'; m_{\rm N})$. The normalization factor, $\sqrt{Z}$, is the coupling strength of the composite operator $\hat{N}(x)$ to the physical nucleon state.

Through the NZ reduction formula, the BS amplitude in equation (1) is related to the four-point Green's function G_4 of the composite nucleons, which is decomposed into the free part and the scattering part, $G_4 = Z^2(G_4^{(0)} + G_4^{(\rm sc)})$, where $G_4^{(0)}$ is proportional to a product of the free nucleon propagators. After taking the equal time limit, $x^0 = y^0 = t$, with $\vec{r} \equiv \vec{x} - \vec{y}$, it is straightforward to rewrite equation (1) as the following integral equation in the center of mass (CM) frame ($\vec{q}' = -\vec{q}$) [20]:

$$\Psi_{\alpha\beta}(\vec{r}, t) = \psi_{\alpha\beta}(\vec{r}; \vec{q}, s, s')\, \mathrm{e}^{-2\mathrm{i}\sqrt{\vec{q}^2 + m_{\rm N}^2}t}, \tag{5}$$

$$\begin{aligned}\psi_{\alpha\beta}(\vec{r}; \vec{q}, s, s') &= Z u_\alpha(\vec{q}, s) u_\beta(-\vec{q}, s') \mathrm{e}^{\mathrm{i}\vec{q}\cdot\vec{r}} \\ &\quad + Z \sum_{\gamma\delta} \int \frac{\mathrm{d}^3 k}{(2\pi)^3}\, \mathrm{e}^{\mathrm{i}\vec{k}\cdot\vec{r}}\, \mathcal{F}_{\alpha\beta;\gamma\delta}(\vec{k}; \vec{q}) u_\gamma(\vec{q}, s) u_\delta(-\vec{q}, s').\end{aligned} \tag{6}$$

Here $u_\alpha(\vec{q}; s)$ is the positive-energy plain-wave solution of the Dirac equation, and $\mathcal{F}_{\alpha\beta;\gamma\delta}(\vec{k}; \vec{q})$ is an integral kernel obtained from $G_4^{(\rm sc)}$ after carrying out the k_0-integration. Hereafter, we call $\psi_{\alpha\beta}(\vec{r}; \vec{q}, s, s')$ as the BS wavefunction. The differential form of the above equation is obtained by multiplying equation (6) by $(\vec{q}^2 + \nabla^2)/m_{\rm N}$:

$$\frac{1}{m_{\rm N}}(\vec{q}^2 + \nabla^2)\psi_{\alpha\beta}(\vec{r}; \vec{q}, s, s') = K_{\alpha\beta}(\vec{r}; \vec{q}, s, s'). \tag{7}$$

Note that we have not made any non-relativistic approximation to derive equation (7). An important observation is that the plain-wave component of $\psi_{\alpha\beta}(\vec{r}; \vec{q}, s, s')$ is projected out by the operator $(\vec{q}^2 + \nabla^2)$ so that the function $K_{\alpha\beta}(\vec{r}; \vec{q}, s, s')$ is localized in coordinate space as long as $|\vec{q}|$ stays below the inelastic threshold as noted for pion–pion scattering in [22]. This is equivalent to saying that the Fourier transform of K with respect to $\vec{r}$, which is proportional to the half off-shell T-matrix relating the on-shell state to momentum $\vec{q}$ and the off-shell state to momentum $\vec{k}$, does not develop a real pole as a function of $|\vec{k}|$, if $|\vec{q}|$ is below the inelastic threshold.

3. The nucleon–nucleon potential

In an abbreviated notation, $(\vec{r}, \alpha, \beta) \to x$ and $(\vec{q}, s, s') \to q$, equation (7) is written as

$$(E_q - H_0)\psi(x; q) = K(x; q), \tag{8}$$

where $E_q = \vec{q}^2/m_{\rm N}$ and $H_0 = -\nabla^2/m_{\rm N}$. This equation defined in a finite box can be used to extract various information on the NN scattering from the lattice QCD simulations.

(i) Consider $K(x; q)$ as a measure to identify the length R beyond which the two nucleons do not interact. If we stay in such a region where $K(x > R; q) \simeq 0$, the wavefunction $\psi(x > R; q)$ can be expanded by the solution of the Helmholtz equation inside a finite box. Then one can extract the phase shift given the incoming energy E_q. This is the approach originally proposed in [23] and is later elaborated to study hadron–hadron scatterings on the lattice [22, 24–26].

(ii) Alternatively, one may extract the half off-shell T-matrix in momentum space by calculating the left-hand side of equation (8) in the coordinate space and making Fourier transform with respect to x.

(iii) One can go one step further and define the non-local NN potential $U(x, x')$ from $K(x; q)$, so that equation (8) becomes the Schrödinger-type equation.

If we are interested only in the NN scattering phase shift in the free space, procedure (i) is certainly enough. In contrast, if we are interested in applying equation (8) to the problems of bound states and the nuclear many-body system, procedures (ii) and (iii) are useful since they give us the off-shell information in a well-defined manner in QCD. To see this explicitly for case (iii), we introduce a set of functions labeled by q, $\{\tilde{\psi}(x; q)\}$, which is dual to the set $\{\psi(x; q)\}$ in the following sense:

$$\int \mathrm{d}x\, \tilde{\psi}(x; q)\psi(x; p) = \delta_{q,p}. \tag{9}$$

As long as the dimensions of the x-space and p-space are the same and the elements in $\{\psi(x; p)\}$ are linearly independent, such a dual basis exists and is unique. If the dimension of p-space is less than that of x-space, the dual basis exists but is not unique[8]. Assuming the existence (but not necessarily the uniqueness) of the dual basis, the non-local potential can be defined as

$$U(x, x') = \int \mathrm{d}p\, K(x, p)\tilde{\psi}(x'; p). \tag{10}$$

Equations (9) and (10) lead to the formula, $K(x; q) = \int \mathrm{d}x' U(x, x')\psi(x'; q)$, so that equation (8) becomes

$$\frac{-\nabla^2}{m_{\mathrm{N}}}\psi_{\alpha\beta}(\vec{r}; \vec{q}, s, s') + \int \mathrm{d}^3r'\, U_{\alpha\beta;\gamma\delta}(\vec{r}, \vec{r}')\psi_{\gamma\delta}(\vec{r}'; \vec{q}, s, s') = E_q\psi_{\alpha\beta}(\vec{r} : \vec{q}, s, s'). \tag{11}$$

Note that the non-local potential U can be rewritten in the form

$$U(\vec{r}, \vec{r}') = V(\vec{r}, \nabla)\delta(\vec{r} - \vec{r}'). \tag{12}$$

The general structure of $V(\vec{r}, \nabla)$ under various symmetry constraints in the non-relativistic kinematics has been worked out by Okubo and Marshak [27]. If we further make the derivative expansion at low energies [28], we will obtain the expression familiar in the phenomenological potentials acting on the upper components of the wavefunction;

$$\begin{aligned} V(\vec{r}, \nabla) = {} & V_0(r) + V_\sigma(r)(\vec{\sigma}_1 \cdot \vec{\sigma}_2) + V_\tau(r)(\vec{\tau}_1 \cdot \vec{\tau}_2) + V_{\sigma\tau}(r)(\vec{\sigma}_1 \cdot \vec{\sigma}_2)(\vec{\tau}_1 \cdot \vec{\tau}_2) \\ & + V_{\mathrm{T}}(r)S_{12} + V_{\mathrm{T}\tau}(r)S_{12}(\vec{\tau}_1 \cdot \vec{\tau}_2) + V_{\mathrm{LS}}(r)(\vec{L} \cdot \vec{S}) + V_{\mathrm{LS}\tau}(r)(\vec{L} \cdot \vec{S})(\vec{\tau}_1 \cdot \vec{\tau}_2) + O(\nabla^2). \end{aligned} \tag{13}$$

Here $S_{12} = 3(\vec{\sigma}_1 \cdot \vec{n})(\vec{\sigma}_2 \cdot \vec{n}) - \vec{\sigma}_1 \cdot \vec{\sigma}_2$ is the tensor operator with $\vec{n} = \vec{r}/|\vec{r}|$, $\vec{S} = (\vec{\sigma}_1 + \vec{\sigma}_2)/2$ the total spin operators, $\vec{L} = -\mathrm{i}\vec{r} \times \nabla$ the orbital angular momentum operator, and $\vec{\tau}_{1,2}$ are the isospin operators for the nucleons. Each component of the potential in equation (13) can be obtained by appropriate spin, isospin and angular momentum projection of the BS wavefunction. Also, the higher derivative terms of the potential in equation (13) can be deduced by combining the BS wavefunctions for different incident energies.

It is appropriate here to remark that the structure of the non-local potential $U(x, x')$ is directly related to the nucleon interpolating operator adopted in defining the BS wavefunction. Different choices of the interpolating operator would give different forms of the NN potential at short distances, although they give the same phase shift at asymptotic large distances. The advantage of working in QCD is that we can unambiguously trace the connection between the NN potential and the interpolating operator.

[8] This can be explained easily as follows. Let us introduce a basis $\{\mathbf{e}_{(1)}, \mathbf{e}_{(2)}, \ldots, \mathbf{e}_{(N)}\}$ in the N-dimensional vector space. The BS wavefunction in discretized coordinates $\psi(x; p) \equiv \psi(i; \alpha)$ corresponds to $\mathrm{e}^{\mathrm{i}}_{(\alpha)}$ with $1 \leqslant \mathrm{i} \leqslant N$ and $1 \leqslant \alpha \leqslant M \leqslant N$. If $M = N$, there exists a unique dual basis, $\{\tilde{\mathbf{e}}_{(1)}, \tilde{\mathbf{e}}_{(2)}, \ldots, \tilde{\mathbf{e}}_{(N)}\}$, satisfying $\tilde{\mathbf{e}}_{(\alpha)} \cdot \mathbf{e}_{(\beta)} = \delta_{\alpha\beta}$ (see any textbook of linear algebra). If $M < N$, there is still a dual basis $\{\tilde{\mathbf{e}}_{(1)}, \tilde{\mathbf{e}}_{(2)}, \ldots, \tilde{\mathbf{e}}_{(M)}\}$ satisfying the above condition for $\alpha \leqslant M$ and $\beta \leqslant M$. However, it is not unique, because one always has the freedom to add linear combinations of $\tilde{\mathbf{e}}_\gamma$ $(M + 1 \leqslant \gamma \leqslant N)$ to the above dual basis.

4. Effective central potential on the lattice

The BS wavefunction in the S-wave on the lattice with the lattice spacing a and the spatial lattice volume L^3 is obtained by

$$\psi(r) = \frac{1}{24}\sum_{R\in O}\frac{1}{L^3}\sum_{\vec{x}} P^{\sigma}_{\alpha\beta}\left\langle 0\left|\hat{n}_\beta(R[\vec{r}]+\vec{x})\hat{p}_\alpha(\vec{x})\right|\mathrm{pn};q\right\rangle. \tag{14}$$

The summation over $R\in O$ is taken for the cubic transformation group to project out the S-wave[9]. The summation over $\vec{x}$ is for selecting the state with zero total momentum. We take the upper components of the Dirac indices to construct the spin singlet (triplet) channel by $P^{\sigma=\mathrm{singlet}}_{\alpha\beta} = (\sigma_2)_{\alpha\beta}$ ($P^{\sigma=\mathrm{triplet}}_{\alpha\beta} = (\sigma_1)_{\alpha\beta}$). The BS wavefunction $\psi(\vec{r})$ is understood as the probability amplitude to find 'neutron-like' three-quarks located at point $\vec{x}+\vec{r}$ and 'proton-like' three-quarks located at point $\vec{x}$.

In the actual simulations, the BS wavefunction is obtained from the four-point correlator,

$$G_4(\vec{x},\vec{y},t;t_0) = \left\langle 0\left|\hat{n}_\beta(\vec{y},t)\hat{p}_\alpha(\vec{x},t)\bar{\mathcal{J}}_{pn}(t_0)\right|0\right\rangle = \sum_n A_n\left\langle 0\left|\hat{n}_\beta(\vec{y})\hat{p}_\alpha(\vec{x})\right|n\right\rangle \mathrm{e}^{-E_n(t-t_0)}. \tag{15}$$

Here $\bar{\mathcal{J}}_{pn}(t_0)$ is a wall source located at $t{=}t_0$, which produces the two nucleons with zero total momentum. The eigen-energy and the eigen-state of the six-quark system are denoted by E_n and $|n\rangle$, respectively, with the matrix element $A_n(t_0){=}\langle n|\bar{\mathcal{J}}_{pn}(t_0)|0\rangle$. For $(t-t_0)/a{\gg}1$, the G_4 and hence the wavefunction ψ are dominated by the lowest energy state.

The lowest energy state created by the wall source $\bar{\mathcal{J}}_{pn}(t_0)$ contains not only the S-wave component but also the D-wave component induced by the tensor force. In principle, they can be disentangled by preparing appropriate operator sets for the sink. Study along this line to extract the mixing between the S-wave and the D-wave at low energies has been put forward recently in [29]. In the present paper, instead of making such a decomposition, we define an 'effective' central potential $V_{\mathrm{C}}(r)$ according to [15, 16] as follows:

$$V_{\mathrm{C}}(r) = E_q + \frac{1}{m_{\mathrm{N}}}\frac{\nabla^2\psi(r)}{\psi(r)}. \tag{16}$$

Note that one can test the non-locality of the potential $U(x,x')$ by evaluating the effective central potential for different energies. If there arises appreciable energy dependence of $V_{\mathrm{C}}(r)$, it is a signature of the necessity of high derivative terms in equation (13).

5. Setup of the lattice simulations

In lattice QCD simulations, the vacuum expectation value of an operator $\mathcal{O}(q,\bar{q},U)$ is defined as

$$\begin{aligned}\langle\mathcal{O}\rangle &= \mathcal{Z}^{-1}\int\prod_\ell \mathrm{d}U(\ell)\prod_x \mathrm{d}q(x)\mathrm{d}\bar{q}(x)\mathcal{O}(q,\bar{q},U)\,\mathrm{e}^{-S_{\mathrm{f}}(q,\bar{q},U)-S_{\mathrm{g}}(U)}\\ &= \mathcal{Z}^{-1}\int\prod_\ell \mathrm{d}U(\ell)\,Q(U)\det M(U)\,\mathrm{e}^{-S_{\mathrm{g}}(U)}.\end{aligned} \tag{17}$$

where $\mathcal{Z} = \int\prod_\ell \mathrm{d}U(\ell)\prod_x \mathrm{d}q(x)\mathrm{d}\bar{q}(x)\,\mathrm{e}^{-S_{\mathrm{f}}(q,\bar{q},U)-S_{\mathrm{g}}(U)}$ is the QCD partition function, $S_{\mathrm{f}} = \sum_{x,x'}\bar{q}(x)M_{xx'}(U)q(x')$ is the quark part of the action, and S_{g} is the gluon part of the action. The quark field $q(x)$ is defined on each site x of the hypercubic space–time lattice, whereas the gluon field $U(\ell)$ denoted by a 3×3 special unitary matrix is defined on each link ℓ. In equation (17), the integration of the quark fields is carried out analytically. In the quenched approximation adopted in our simulation, the virtual fermion loop denoted by

[9] In principle, this projection cannot remove possible contamination from the higher orbital waves with $L \geqslant 4$, although these contributions are expected to be negligible.

Table 1. The number of gauge configurations $N_{\rm conf}$, the pion mass m_π, the nucleon mass $m_{\rm N}$ and the time-slice $t - t_0$ on which BS wavefunctions are measured, and the non-relativistic energies $E_q \equiv q^2/m_{\rm N}$ for ${}^1S_0$ and ${}^3S_1$ channels.

κ	$N_{\rm conf}$	m_π (MeV)	$m_{\rm N}$ (MeV)	$(t-t_0)/a$	$E_q({}^1S_0)$ (MeV)	$E_q({}^3S_1)$ (MeV)
0.1640	1000	732.1 (4)	1558.4 (63)	7	−0.400 (83)	−0.480 (97)
0.1665	2000	529.0 (4)	1333.8 (82)	6	−0.509 (94)	−0.560 (114)
0.1678	2021	379.7 (9)	1196.6 (32)	5	−0.675 (264)	−0.968 (374)

$\det M(U)$ is set as 1 and the integration over link variables U is performed using the importance sampling method[10].

We employ the standard plaquette gauge action on a 32^4 lattice with the bare QCD coupling constant $\beta = 6/g^2 = 5.7$. The corresponding lattice spacing is determined to be $1/a = 1.44(2)$ GeV ($a \simeq 0.137$ fm) from the ρ meson mass in the chiral limit [31]. Then, the physical size of our lattice becomes $L \simeq 4.4$ fm. For the fermion action, we adopt the standard Wilson quark action with the hopping parameter ($\kappa = 0.1640$, 0.1665 and 0.1678) which controls the quark masses. The periodic (Dirichlet) boundary condition is imposed on the quark fields along the spatial (temporal) direction. To generate the quenched gauge configurations, we adopt the heatbath algorithm with overrelaxation and sample configurations are taken in every 200 sweeps after skipping 3000 sweeps for thermalization.

For our numerical simulations, we use IBM Blue Gene/L at KEK, which consists of 10 240 computation nodes with total theoretical performance of 57.3 TFlops. A modified version of the CPS ++ (the Columbia Physics System) [33] is used to generate quenched gauge configurations and propagators of quarks. Most of the computational time is devoted to the calculation of the four-point function of nucleons, for which our code achieves 34–48% of peak performance. Totally ∼4000 h are used by queues with 512 nodes for the calculations of the effective central potentials corresponding to the three values of hopping parameters. The number of sampled gauge configurations $N_{\rm conf}$, the pion mass m_π and the nucleon mass $m_{\rm N}$ are summarized in table 1. (For κ=0.1678, we have removed 24 exceptional gauge configurations from the sample.)

We adopt the wall source on the time-slice $t/a = t_0/a = 5$. The BS wavefunctions are measured on the time-slice $(t - t_0)/a = 7, 6, 5$ for $\kappa = 0.1640$, 0.1646 and 0.1678, respectively. The ground-state saturation is examined by the t-dependence of the NN potential. We employ the nearest-neighbor representation of the discretized Laplacian as $\nabla^2 f(\vec{x}) \equiv \sum_{i=1}^{3}\{f(\vec{x} + a\vec{n}_i) + f(\vec{x} - a\vec{n}_i)\} - 6f(\vec{x})$, where $\vec{n}_i$ denotes the unit vector along the ith coordinate axis. BS wavefunctions are fully measured for $r < 0.7$ fm, where rapid change of the NN potential is expected. Since the change is rather modest for $r > 0.7$ fm, the measurement of BS wavefunctions is restricted on the coordinate axes and their nearest neighbors to reduce the calculational cost. The 'asymptotic momentum' q is obtained by fitting the BS wavefunction with Green's function in a finite and periodic box [23]:

$$G(\vec{r}; q^2) = \frac{1}{L^3}\sum_{\vec{n}\in\mathbf{Z}^3}\frac{\mathrm{e}^{\mathrm{i}(2\pi/L)\vec{n}\cdot\vec{r}}}{(2\pi/L)^2\vec{n}^2 - q^2}, \tag{18}$$

which satisfies $(\nabla^2 + q^2)G(\vec{r}; q^2) = -\delta_L(\vec{r})$ with $\delta_L(\vec{r})$ being the periodic delta-function. In the actual calculation, equation (18) is rewritten in terms of the heat kernel $\mathcal{H}$ satisfying the heat equation, $\partial_t\mathcal{H}(t, \vec{r}) = \nabla^2\mathcal{H}(t, \vec{r})$, with the initial condition, $\mathcal{H}(t \to 0+, \vec{r}) = \delta_L(\vec{r})$. The fits are performed outside the range of NN interaction determined by $\nabla^2\psi(\vec{r})/\psi(\vec{r})$ [25].

6. Numerical results

Figure 2 (upper panel) shows the BS wavefunctions in ${}^1S_0$ and ${}^3S_1$ channels for $\kappa = 0.1665$. The suppression of the wavefunction in the region $r < 0.5$ fm indicates the existence of repulsion at short distances. Figure 2

[10] For various simulation techniques in lattice gauge theories, see e.g. [30].

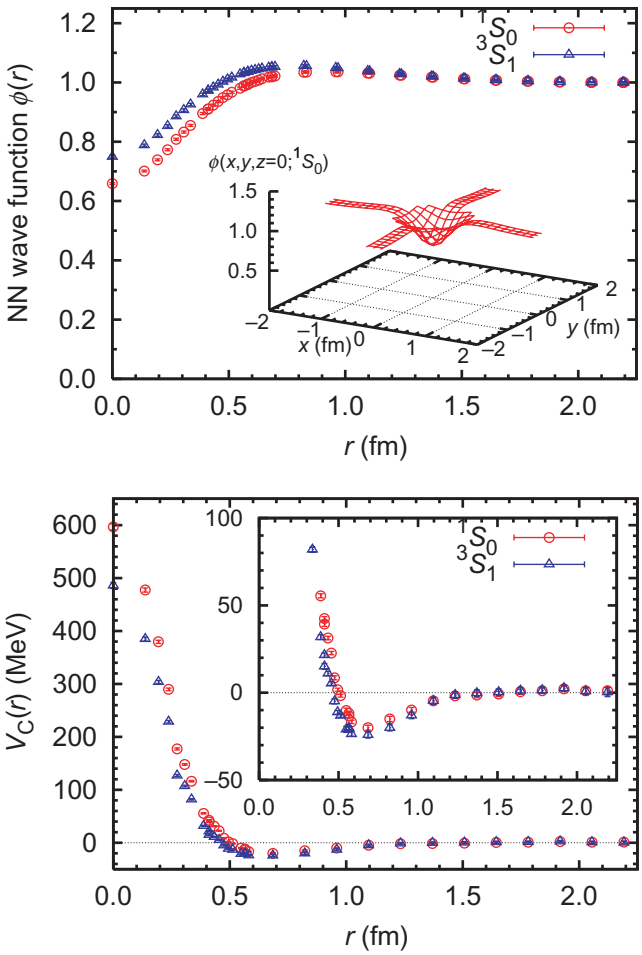

Figure 2. Upper panel: the NN wavefunctions in $^1S_0$ and $^3S_1$ channels. The inset is a three-dimensional (3D) plot of the wavefunction $\phi(x, y, z = 0; ^1S_0)$. Lower panel: the NN effective central potential in the $^1S_0$ and $^3S_1$ channels for $m_\pi = 529$ MeV ($\kappa = 0.1665$).

(lower panel) shows the reconstructed NN potentials for $\kappa = 0.1665$, i.e. the effective central potentials for $^1S_0$ and $^3S_1$ channels. See table 1, for the values of the non-relativistic energies $E_q \equiv q^2/m_{\rm N}$ in equation (16).

We show the NN potentials for three different quark masses in $^1S_0$ channel in figure 3. As the quark mass decreases, the repulsive core at short distances is enhanced rapidly, whereas the attraction at medium distances is modestly enhanced. This indicates that it is important to perform the lattice QCD calculations for the lighter quark mass region in order to make quantitative comparison of our results with the observables in the real world.

Although there exist both attraction and repulsion, the net effect of our potential is attractive at low energies as shown by the scattering lengths calculated from Lüscher's formula in table 2 [23]. The attractive nature of our potential is qualitatively understood by the Born approximation formula for the scattering length $a_0 \simeq -m_N \int V_{\rm C}(r) r^2 \, {\rm d}r$. Owing to the volume factor $r^2 \, {\rm d}r$, the attraction at medium distances can overcome the repulsive core at short distances. However, there is a considerable discrepancy between the scattering lengths in table 2 and the empirical values, $a_0^{(\rm exp)}(^1S_0) \sim 20$ fm and $a_0^{(\rm exp)}(^3S_1) \sim -5$ fm. This is attributed to the heavy quark masses employed in our simulations.

If we can get closer to the physical quark mass, there appears a 'unitary region' where the NN scattering length becomes singular and changes sign as a function of the quark mass [26, 31, 32]. The singularity is associated with the formation of the di-nucleon bound state. Because of this, the NN scattering length becomes a highly nonlinear function of the light quark mass. One should note that the NN potential changes smoothly

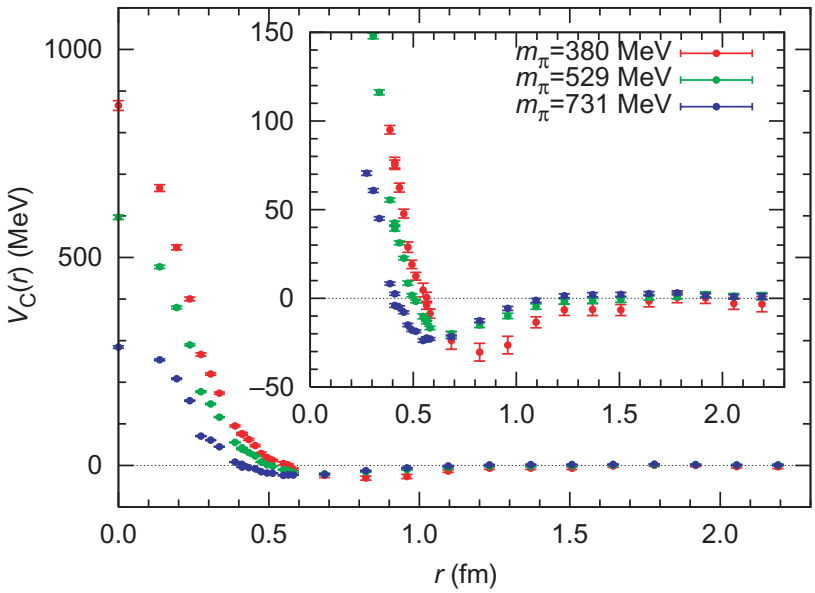

Figure 3. Central potentials in the $^1S_0$ channel for three different quark masses in the quenched QCD simulations on a $(4.4\,\mathrm{fm})^4$ lattice.

Table 2. Scattering lengths obtained from Lüscher's formula [23] in the spin-singlet and spin-triplet channels for different quark masses.

κ	m_π (MeV)	$a_0(^1S_0)$ (fm)	$a_0(^3S_1)$ (fm)
0.1640	732.1 (4)	0.115 (26)	0.140 (31)
0.1665	529.0 (4)	0.126 (25)	0.140 (31)
0.1678	379.7 (9)	0.159 (66)	0.252 (104)

even in the unitary region in contrast with the scattering length. This is one of the reasons why the NN potential is a much more appropriate quantity to be examined on the lattice instead of the NN scattering length.

7. Summary and concluding remarks

In this paper, we have outlined the basic notion of the NN potential and its field-theoretical derivation from the equal-time BS amplitude. Such a formulation allows us to extract the potential between extended objects by using the lattice QCD simulations. The central part of the NN potential at low energies was obtained in lattice QCD simulations with quenched approximation. It was found that the NN potential calculated on the lattice at low energy shows all the basic features expected from the empirical NN potentials determined from the NN scattering data: attraction at long and medium distances and repulsion at short distances. This is the first step toward the understanding of atomic nuclei from the fundamental law of strong interaction, the QCD.

There are many directions to be explored on the basis of our approach.

1. Energy dependence of the NN potential in equation (16) should be studied to test the non-locality of the potential $U(x, x')$ and the validity of its derivative expansion. This is currently being investigated by changing the spatial boundary condition of the fermion field [34].
2. The tensor force, which mixes the states with different orbital angular momenta by two units, is a unique feature of the nuclear force and plays an essential role in the deuteron binding. This is also being investigated by projecting out the $^3S_1$ component and the $^3D_1$ component separately from the exact two-nucleon wavefunction with $J = 1$ on the lattice [29, 35]. The spin–orbit force, which is known to be strong at short distances in empirical NN force, should also be studied.

3. The three-nucleon force is thought to play important roles in nuclear structure and also in the equation of state of high-density matter. Since the experimental information is scarce, simulations of the three nucleons on the lattice combined with appropriate generalizations of the formulae in section 2 may lead to the first principle determination of the three-nucleon potential in the future. With these generalizations of the present approach, one may eventually make a firm link between QCD and the physics of the nuclear structure[11].
4. The YN and hyperon–hyperon (YY) potentials are essential for understanding the properties of hypernuclei and the hyperonic matter inside the neutron stars. However, the experimental data are very limited due to the short lifetime of hyperons. On the lattice, NN, YN and YY interactions can be treated on the same footing since the difference is only the mass of the strange quark. Recently, the ΞN potential [18, 19] and the ΛN potential [37] were examined as a first step toward systematic derivation of the hyperon interactions.
5. To compare the NN potential on the lattice with experimental observables, it is necessary to carry out full QCD simulations that take into account the dynamic quark loops. A study of the nuclear force with the use of the full QCD configurations generated by PACS–CS Collaboration [38] is currently in progress [34, 35, 37].

Acknowledgments

This research work was partly supported by the Ministry of Education, Culture, Sports, Science and Technology of Japan through Grant-in-Aid numbers 18540253, 19540261 and 20340047. Numerical simulations were supported by the Large Scale Simulation Program number 07-07 (FY2007) of the High Energy Accelerator Research Organization (KEK). We are grateful to the authors and maintainers of `CPS++` [33], a modified version of which was used for measurements done in this work.

References

[1] Taketani M *et al* 1967 *Prog. Theor. Phys. Suppl.* **39**
Hoshizaki N *et al* 1968 *Prog. Theor. Phys. Suppl.* **42**
Brown G E and Jackson A D 1976 *Nucleon–Nucleon Interaction* (Amsterdam: North-Holland)
Machleidt R and Slaus I 2001 *J. Phys. G: Nucl. Part. Phys.* **27** R69
[2] http://nn-online.org/
[3] Machleidt R 2001 *Phys. Rev.* C **63** 024001
[4] Wiringa R B, Stoks V G J and Schiavilla R 1995 *Phys. Rev.* C **51** 38
[5] Stoks V G J, Klomp R A M, Terheggen C P F and de Swart J J 1994 *Phys. Rev.* C **49** 2950
[6] Weinberg S 1990 *Phys. Lett.* B **251** 288
Weinberg S 1991 *Nucl. Phys.* B **363** 3
Bedaque P F and van Kolck U 2002 *Annu. Rev. Nucl. Part. Sci.* **52** 339
[7] Machleidt R 1989 *Adv. Nucl. Phys.* **19** 189
[8] Yukawa H 1935 *Proc. Math. Phys. Soc. Japan* **17** 48
[9] Jastrow R 1951 *Phys. Rev.* **81** 165
[10] Tamagaki R *et al* 1993 *Prog. Theor. Phys. Suppl.* **112** 1
Heiselberg H and Pandharipande V 2000 *Annu. Rev. Nucl. Part. Sci.* **50** 481
Lattimer J M and Prakash M 2000 *Phys. Rep.* **333** 121
[11] Wilczek F 2005 *Rev. Mod. Phys.* **77** 857
[12] Myhrer F and Wroldsen J 1988 *Rev. Mod. Phys.* **60** 629
Oka M, Shimizu K and Yazaki K 2000 *Prog. Theor. Phys. Suppl.* **137** 1
Fujiwara Y, Suzuki Y and Nakamoto C 2007 *Prog. Part. Nucl. Phys.* **58** 439
[13] Wilson K G 1974 *Phys. Rev.* D **10** 2445
[14] 2007 *Proc. XXV Int. Symp. on Lattice Field Theory (Regensburg, Germany, 2007) PoS* **LAT2007** 001–389

[11] Reviewed in [36].

[15] Ishii N, Aoki S and Hatsuda T 2007 *Phys. Rev. Lett.* **99** 022001
[16] Ishii N, Aoki S and Hatsuda T 2007 *PoS* **LAT2007** 146 (arXiv:0710.4422 [hep-lat])
[17] Aoki S 2007 *PoS* **LAT2007** 002 (arXiv:0711.2151 [hep-lat])
[18] Nemura H, Ishii N, Aoki S and Hatsuda T 2007 *PoS* **LAT2007** 156 (arXiv:0710.3622 [hep-lat])
[19] Nemura H, Ishii N, Aoki S and Hatsuda T 2008 arXiv:0806.1094 [nucl-th]
[20] Aoki S, Hatsuda T and Ishii N 2008 in preparation
[21] Nishijima K 1958 *Phys. Rev.* **111** 995
Zimmermann W 1958 *Nuovo Cimento* **10** 597
[22] Lin C J D, Martinelli G, Sachrajda C T and Testa M 2001 *Nucl. Phys.* B **619** 467
[23] Lüscher M 1991 *Nucl. Phys.* B **354** 531
[24] Fukugita M, Kuramashi Y, Okawa M, Mino H and Ukawa A 1995 *Phys. Rev.* D **52** 3003
[25] Aoki S *et al* (CP-PACS Collaboration) 2005 *Phys. Rev.* D **71** 094504
[26] Beane S R, Bedaque P F, Orginos K and Savage M J 2006 *Phys. Rev. Lett.* **97** 012001
[27] Okubo S and Marshak R E 1958 *Ann. Phys. NY* **4** 166
[28] Tamagaki R and Watari W 1967 *Prog. Theor. Phys. Suppl.* **39** 23
[29] Ishii N, Aoki S and Hatsuda T 2008 *Mod. Phys. Lett.* A **23** 2281
[30] Rhote H J 2005 *Lattice Gauge Theories: An Introduction* 3rd edn (Singapore: World Scientific)
[31] Kuramashi Y 1996 *Prog. Theor. Phys. Suppl.* **122** 153 (arXiv:hep-lat/9510025)
[32] Epelbaum E, Meissner U G and Gloeckle W 2003 *Nucl. Phys.* A **714** 535
[33] http://qcdoc.phys.columbia.edu/chulwoo_index.html
[34] Aoki A, Balog J, Hatsuda T, Ishii N, Murano K, Nemura H and Weisz P 2008 *XXVI Int. Symp. on Lattice Field Theory (Williamsburg, VA, 2008)*
[35] Ishii N, Aoki S, Hatsuda T and Nemura H (for PACS-CS Collaboration) 2008 *XXVI Int. Symp. on Lattice Field Theory (Williamsburg, VA, 2008)*
[36] Hjorth-Jensen M, Kuo T T S and Osnes E 1995 *Phys. Rep.* **261** 125
Bogner S K, Kuo T T S and Schwenk A 2003 *Phys. Rep.* **386** 1
Weise W 2007 *Prog. Theor. Phys. Suppl.* **170** 161 (arXiv:0704.1992 [nucl-th])
Weise W 2008 *Nucl. Phys.* A **804** 173 (arXiv:0801.1619 [nucl-th])
[37] Nemura H, Ishii N, Aoki S and Hatsuda T (for PACS-CS Collaboration) 2008 *XXVI Int. Symp. on Lattice Field Theory (Williamsburg, VA, 2008)*
[38] Aoki S *et al* (PACS-CS Collaboration) 2008 arXiv:0807.1661 [hep-lat]